Supporting Information

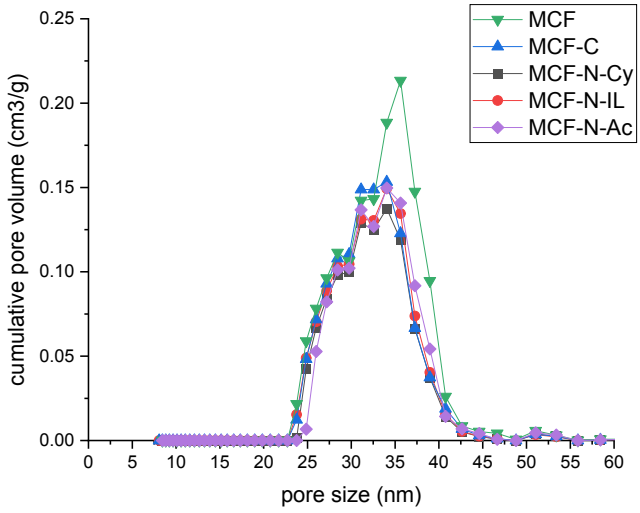

Figure S 1 Pore size distribution of synthesized materials

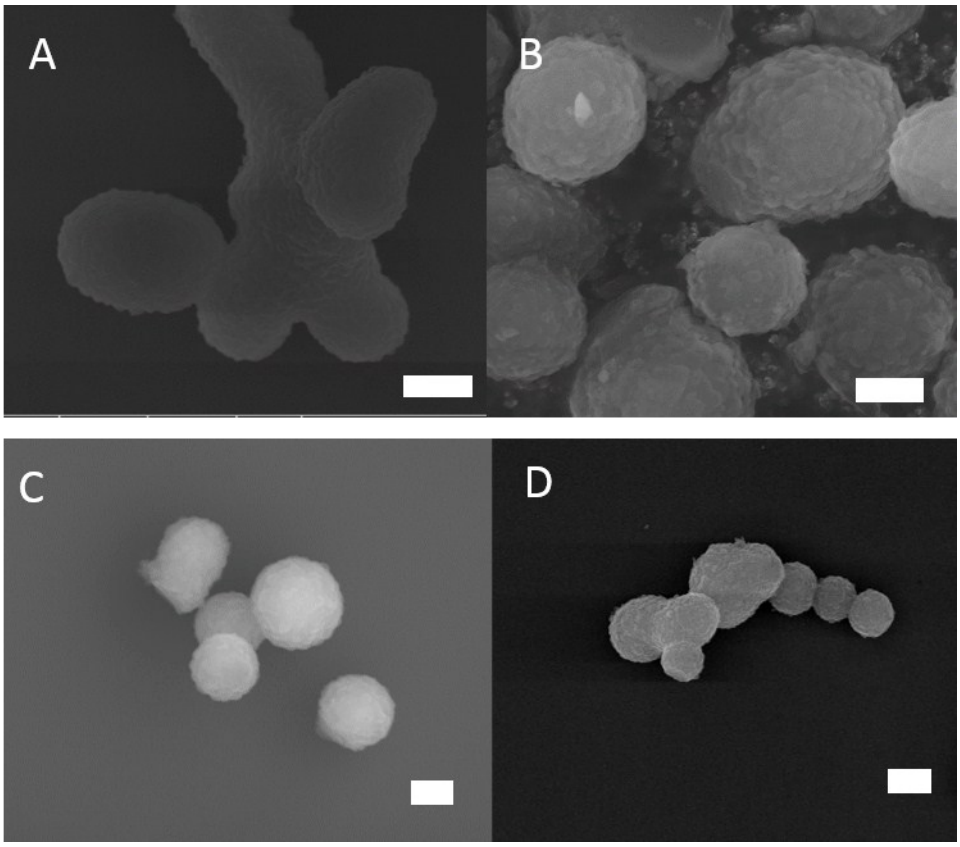

Figure S 2 SEM images of synthesized materials (A) MCF (B) MCF-C (C) MCF-N-Cy (D) MCF-N-IL scale bar- 1µm

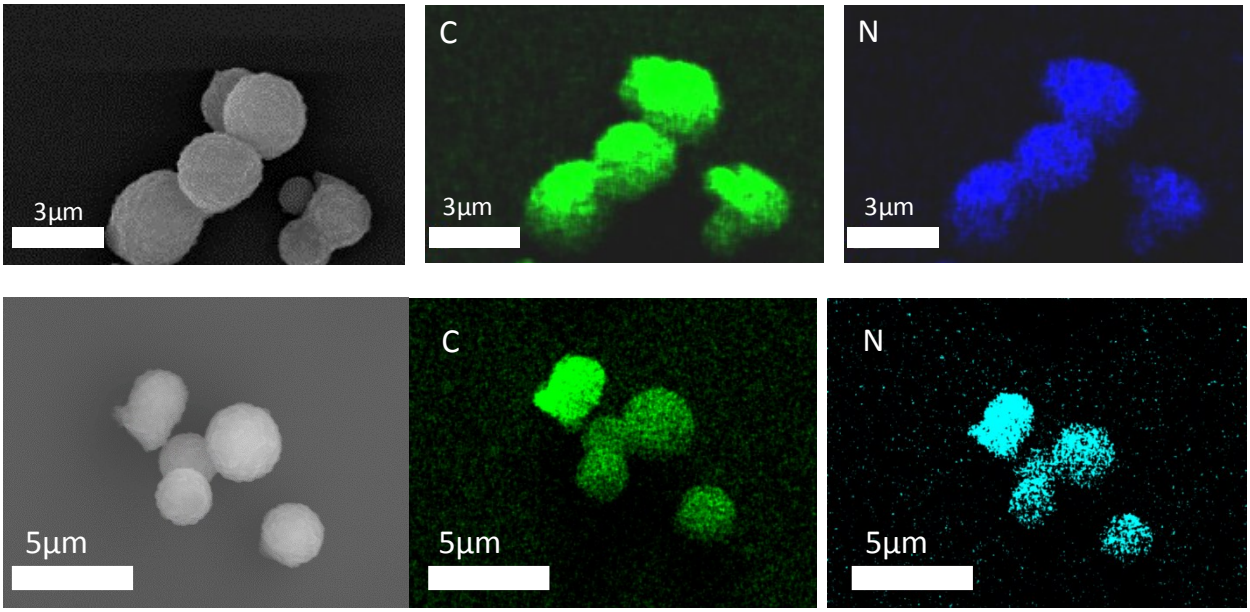

Figure S 3 Elemental mapping of MCF-N-IL (top frame), MCF-N-Cy (bottom frame)

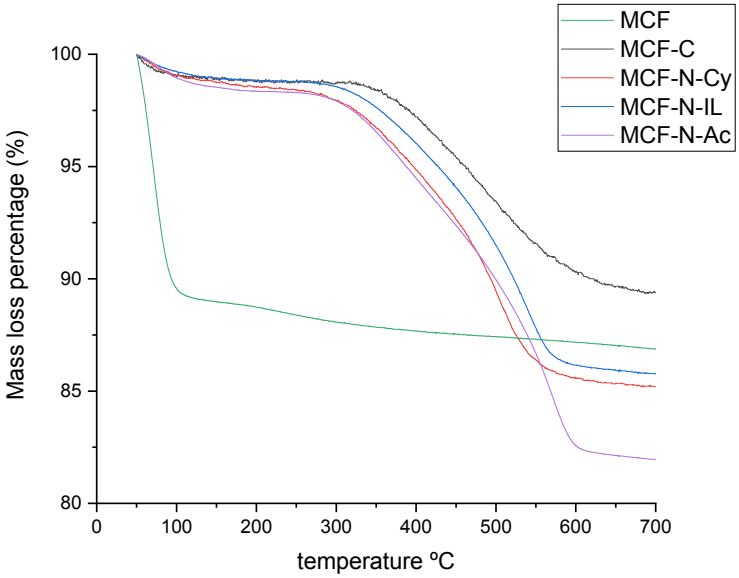

Figure S 4 TGA analyses of synthesized materials

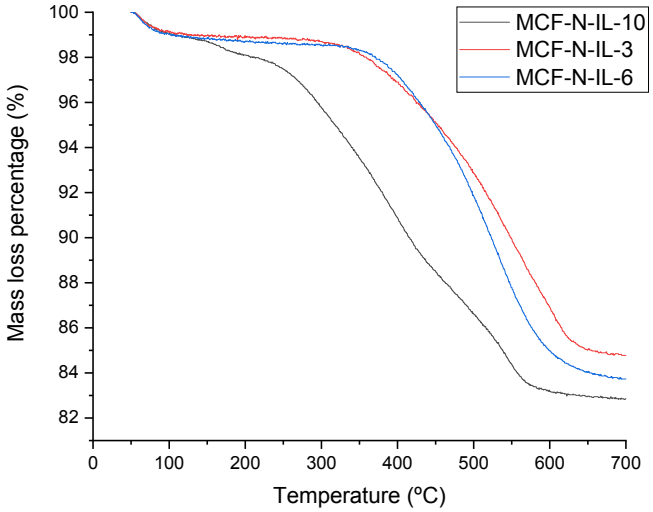

Figure S 5 TGA analyses of MCF-N-IL with different N loading

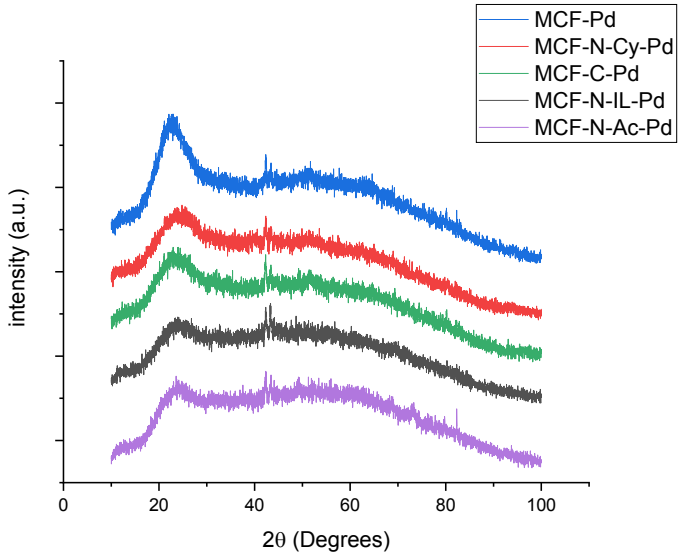

Figure S 6 X-ray diffractgrams of fresh catalysts

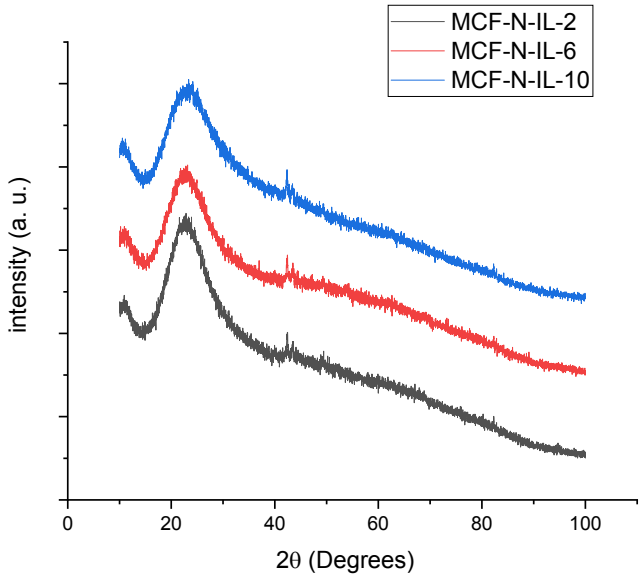

Figure S 7 X-ray diffractgrams of fresh catalysts of MCF-N-IL with different N loading

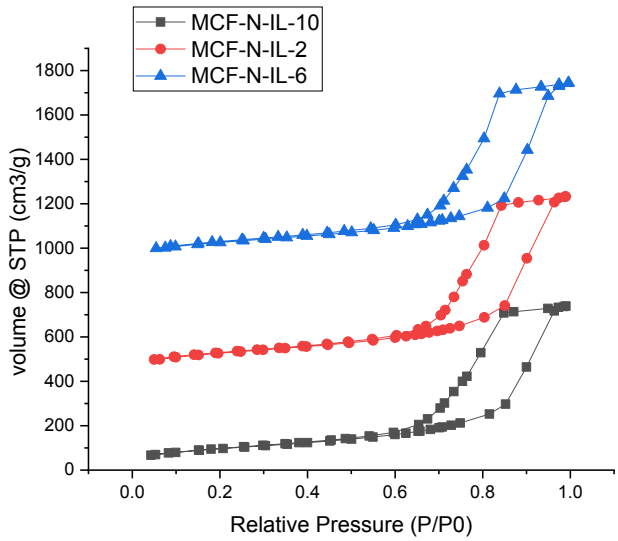

Figure S 8 N2 Physisorption of MCF-N-IL with different N-loading (the isotherm of MCF-N-IL-2 and MCF-N-IL-6 were offset by 400 and 900 respectively)

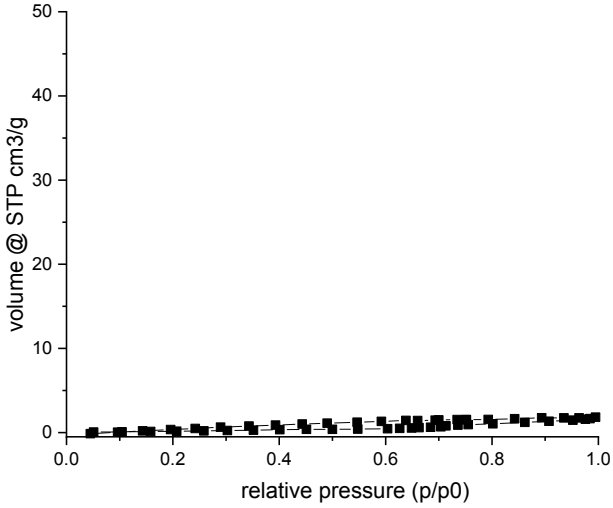

Figure S 9 Physisorption of CN-IL

Table S 1 Structure of CN-IL

Sample	Surface area (m^2/g)	Pore volume (cm^3/g)
CN-IL	1.02	0.003

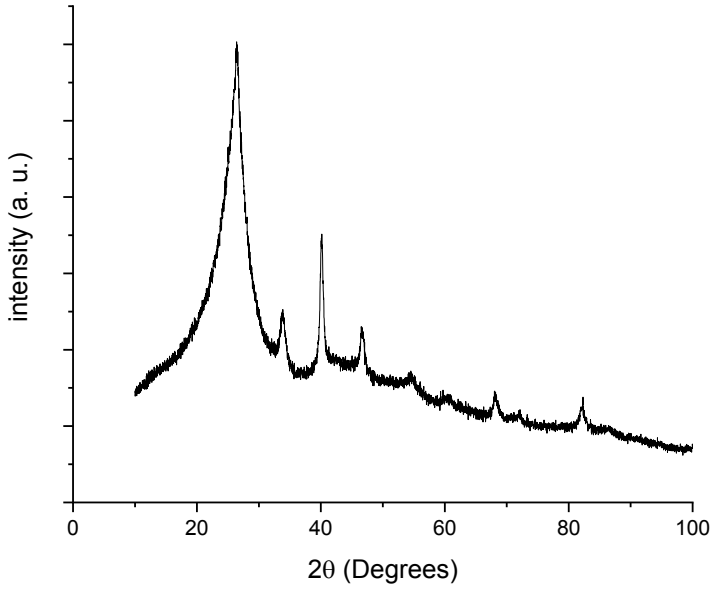

Figure S 10 X-ray diffractgrams of CN-ILPd

Table S 2 Relative abundance percentage of nitrogen types in N 1s XPS spectra

Sample	Component/BE(eV)			
	$N_{pyridinic}$ 398	$N_{pyrrolic}$ 399.7	$N_{graphitic}$ 401	N_{oxides} 402.6

MCF-N-Cy	48.9%	42.4%	8.7%	-
MCF-N-IL	78.9%	15.8%	-	5.3%
MCF-N-AC	35.8%	57.1%	-	7.1%

Table S 3 Relative abundance percentage of palladium types in Pd 3d XPS spectra

sample	Component/BE (eV)	
	Pd^0 335.3	Pd^{2+} 337.5
MCF-Pd	69.9%	30.1%
MCF-C-Pd	50.4%	49.6%
MCF-N-Cy-Pd	41.8%	58.2%
MCF-N-IL-Pd	30.2%	69.8%
MCF-N-IL-Pd	66.13%	33.87%

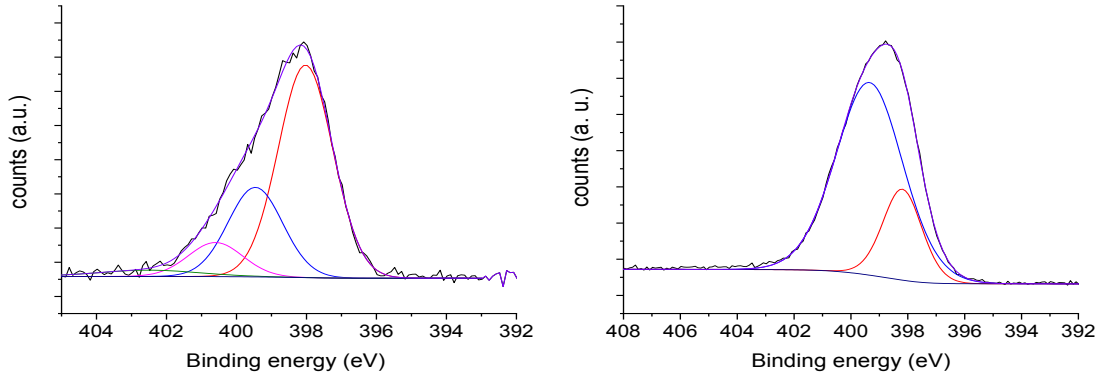

Figure S 11 XPS of N1S of MCF-C-IL-Pd (left) and MCF-N-Cy-Pd (right)

Table S 4 Relative abundance percentage of nitrogen types in N 1s XPS spectra after Pd impregnation

Sample	Component/BE(eV)				
	$N_{pyridinic}$ 398	$N_{pyrrolic}$ 399.7	$N_{graphitic}$ 401	N_{oxides} 402.6	N_{ads} 404.8
MCF-N-Cy-Pd	21.51%	78.49%	-	-	-
MCF-N-IL-Pd	56.1%	29.2%	6.94%	3.75%	4.02%
MCF-N-Ac-Pd	13.57%	75.01%	-	11.42%	-

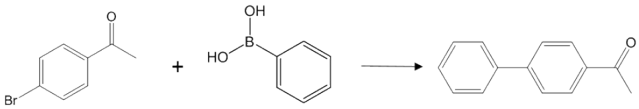

Table S 5 The catalytic performance of MCF-N-IL-Pd

Base	Solvent	Conversion
No Base	Ethanol	8
Et_3N	Ethanol	15
Et_3N	Toluene	5
n-butylamine	Ethanol	21
Piperidine	Ethanol	16
K_2CO_3	Ethanol	99
K_2CO_3	Ethanol	42*

20mg of catalyst (0.75mol% of Pd), 0.5 mmols of 4-bromoacetophenone, 0.7 mmols of phenylboronic acid, 0.5 mmol of base, 4 mLof solvent, 40ºC, 1.0 hour. * using CN-IL-Pd

Table S 6 Pd leaching after Suzuki reaction

Material	Pd leaching %
MCF-Pd	29
MCF-C-Pd	0.5
MCF-N-IL-Pd	Bellow detection limit
MCF-N-Cy-Pd	Bellow detection limit
MCF-N-Ac-Pd	Bellow detection limit

*detection limit 2 ng/ml

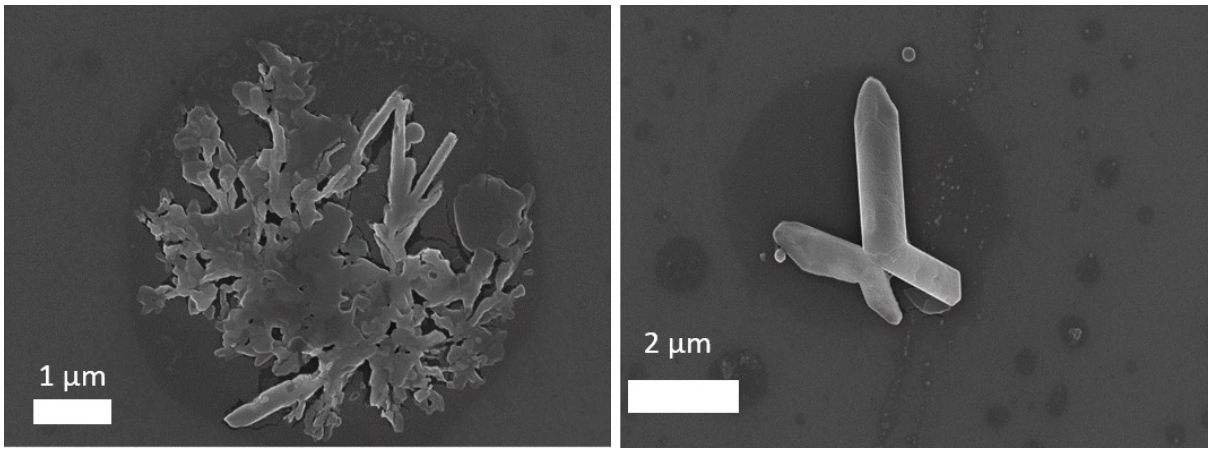

Figure S 12- Spent catalyst (MCF-Pd) after 4 cycles

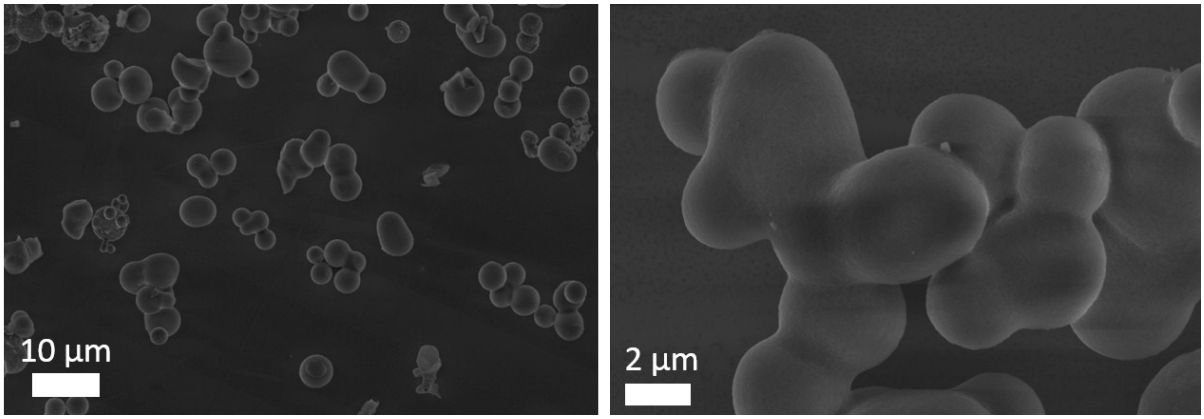

Figure S 13 Spent Catalysts (MCF-C-Pd) after 4 cycles

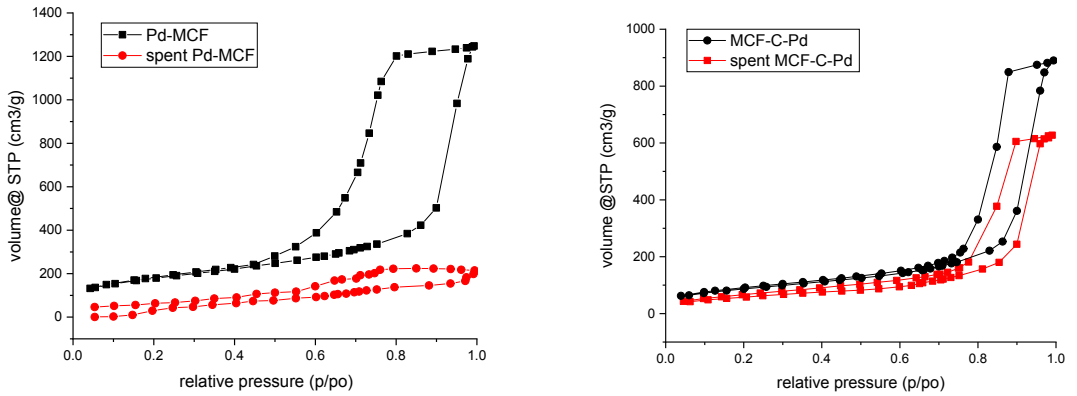

Figure S 14 Nitrogen physisorption isotherms of fresh and spent catalysts

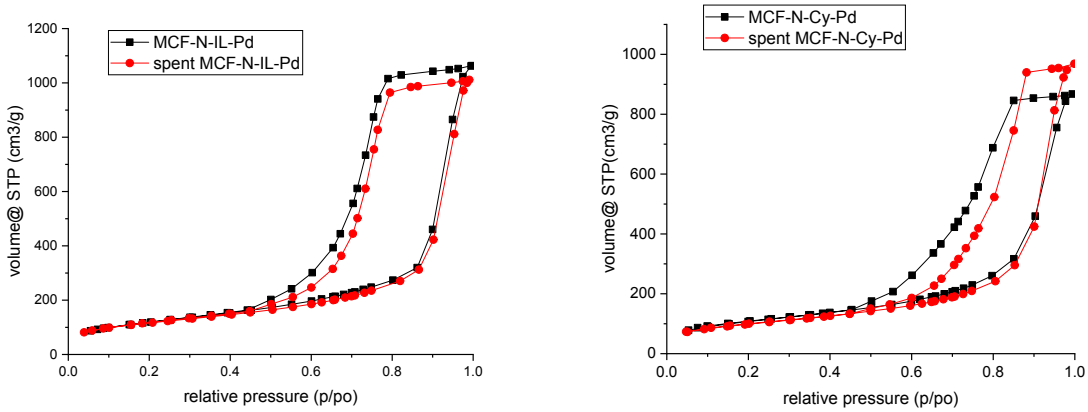

Figure S 15 Nitrogen physisorption isotherms of fresh and spent catalysts

Table S 7 Textural properties of fresh and spent catalysts

Sample	Surface area (m^2/g)	Pore volume (cm^3/g)
Pd-MCF	632	1.85
Spent Pd-MCF	23	0.33
Pd-C- MCF	320	1.32
Spent Pd-C-MCF	216	0.94
MCF-N-IL-Pd	430	1.56
Spent MCF-N-IL-Pd	416	1.48
MCF-N-Cy-Pd	388	1.29
Spent MCF-N-Cy-Pd	357	1.44

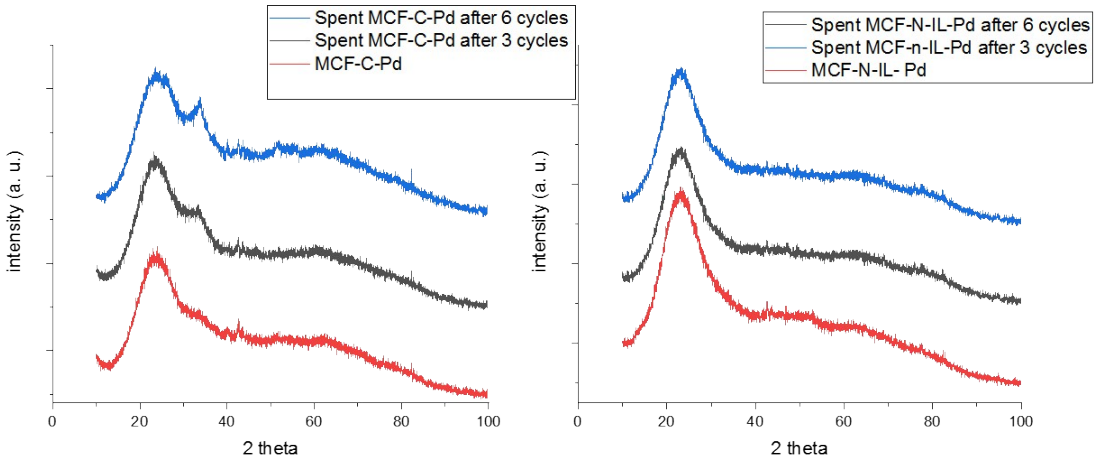

Figure S 16 XRD of fresh and spent catalysts

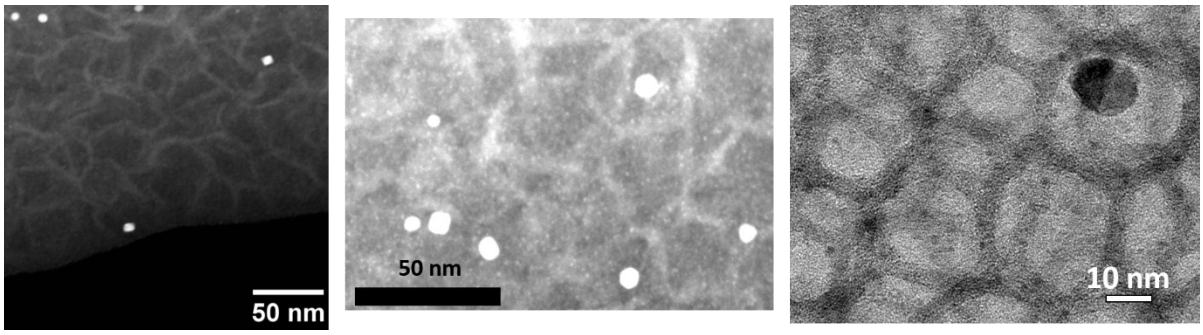

Figure S 17 HAADF-STEM and TEM images of spent MCF-N-IL-Pd after 4 cycles

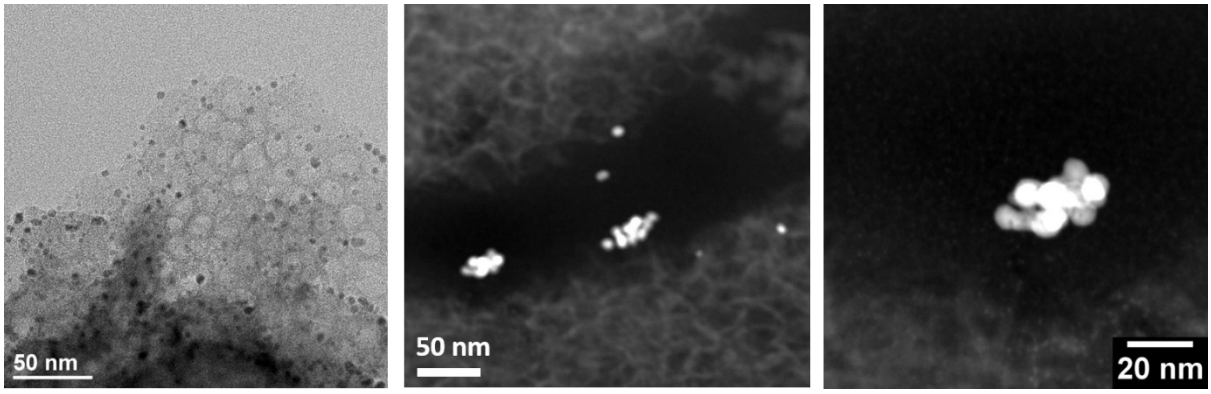

Figure S 18 HAADF-STEM and TEM images of spent MCF-C-Pd after 4 cycles

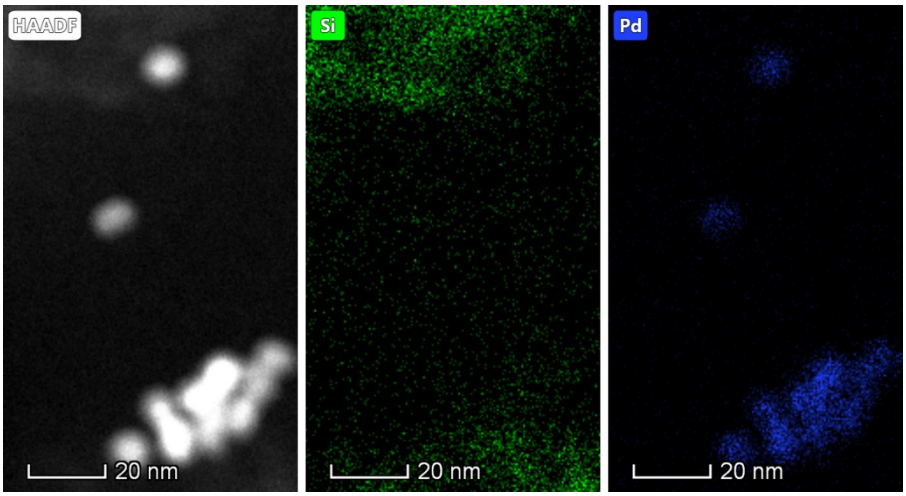

Figure S 19 HAADF-STEM images of spent MCF-C-Pd and elemental mapping

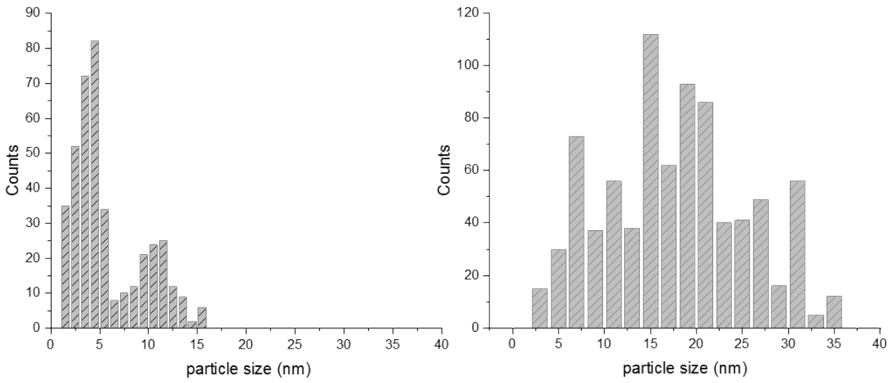

Figure S 20 Histrograms of spent catalysts after 4 cycle of Suzuki reaction MCF-N-IL-Pd (left) and MCF-C-Pd (right)

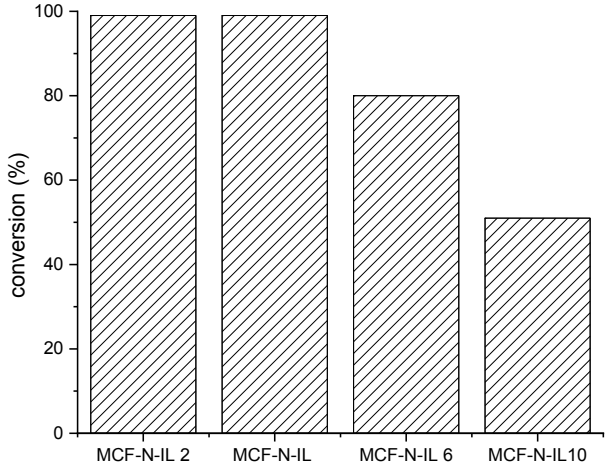

Figure S 21 Influence of N-loading on catalytic activity for the Suzuki reaction

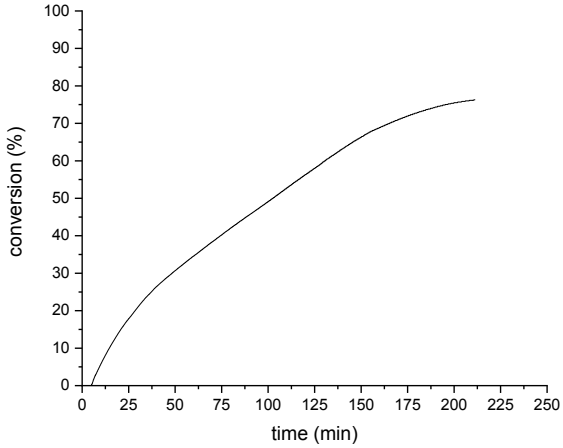

Figure S 22 Catalytic activity CN-IL-Pd for hydrogenation of allyl-benzene

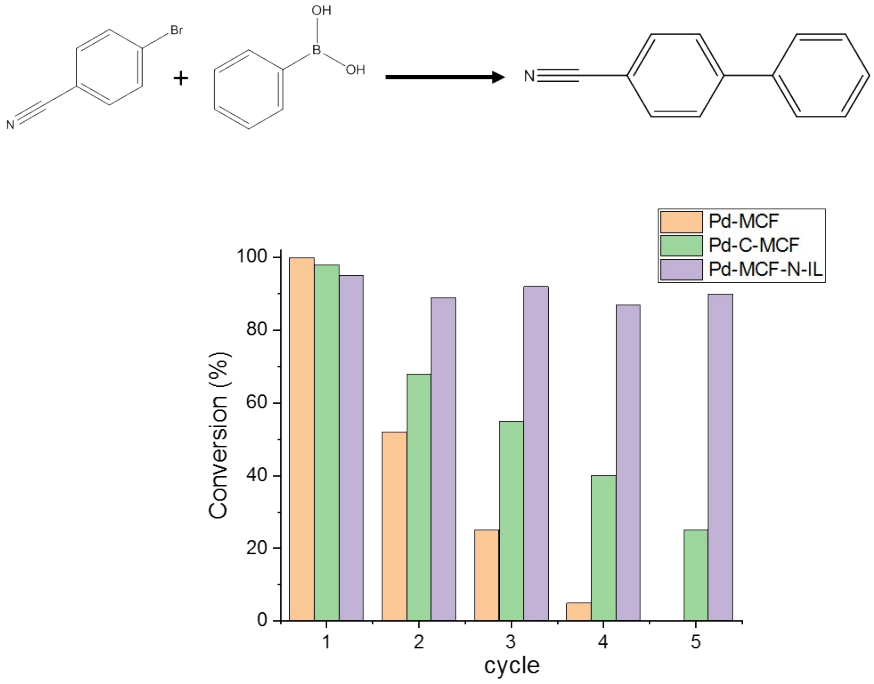

Figure S 23 Recyclability of materials for Suzuki reaction

20mg of catalyst (0.75 mol% of Pd), 0.5 mmols of 4-bromobenzonitrile, 0.7 mmols of phenylboronic acid, 0.5 mmol of K_2CO_3, 4mL EtOH, 40ºC, 1.0 hour

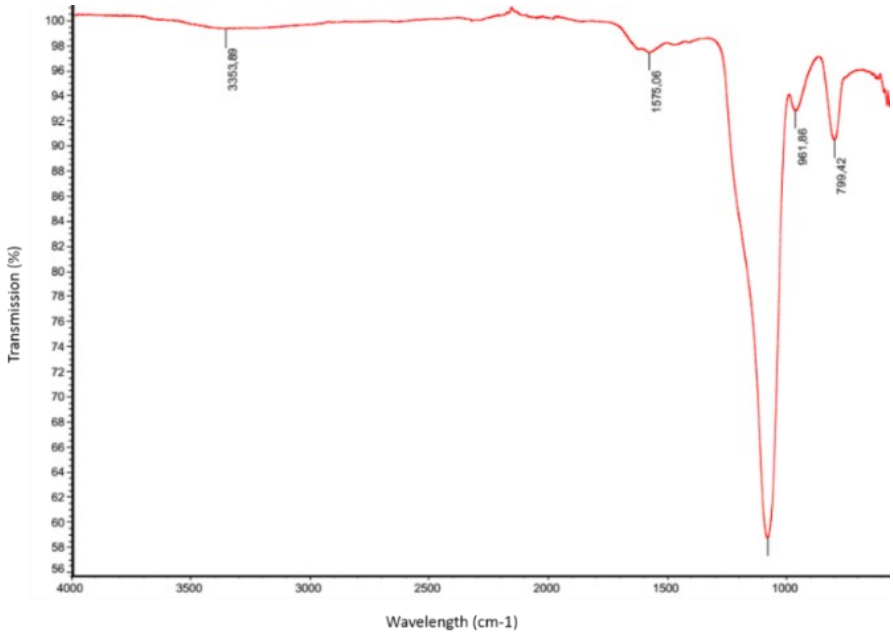

Figure S 24 FT-IR spectra of the MCF-C

The peak at 1575 cm^{-1} corresponds to aromatic ring stretching vibration of furan ring.

Table S 8 Comparison of the catalytic activity heterogeneous catalysts in the Suzuki cross-coupling reaction

Reference	Material	Conditions	Time (h)	Conversion (%)	TOF (h^{-1})*
	This work (MCF-N-IL-Pd)	EtOH/K_2CO_3/40ºC	1	99	133.3
1	SBA-15SHPd	DMF-H_2O/K_2CO_3/80ºC	4.16	98	23.5
2	Fe3O4@SiO2 – iminophosphine- Pd	Toluene/KOH/100ºC	2	93	93
3	GOPPh2	DMF/K_2CO_3/120ºC	6	88	8.6
4	β-cyclodextrin–graphene- Pd	H_2O/Na_2CO_3/90ºC	3	93	154.9
5	Porous glass-Pd	H_2O/Na_2CO_3/150ºC (microwave)	0.16	96	1333
6	GO-NHC-Pd	DMF-H_2O/$CsCO_3$/50ºC	1	88	88
7	MWCNT-Pd	MeOH/CH_3COONa/70ºC	24	100	2.1

*Calculated based on total Pd used in the test

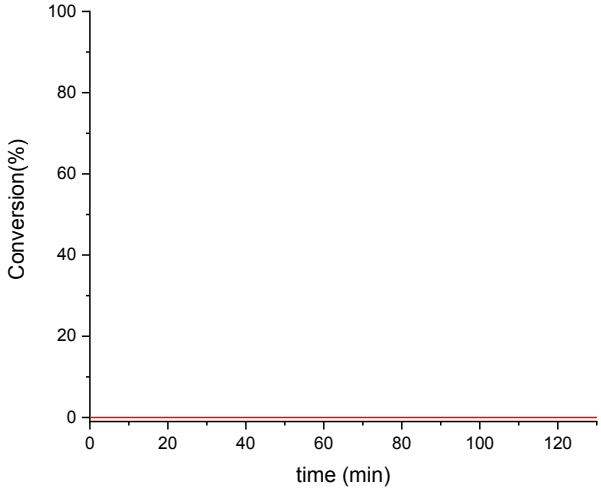

Figure S 25 Conversion versus time of allyl benzene when toluene is used as solvent

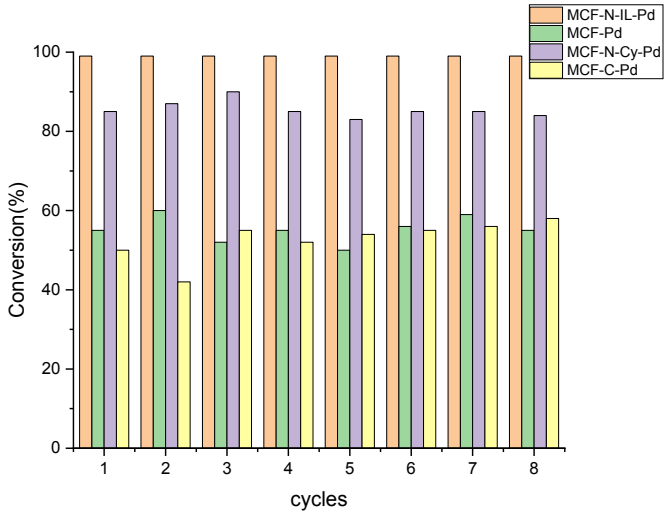

Figure S 26 Recyclability of synthesized catalysts for the hydrogenation of allylbenzene

Table S 9 Comparison of the catalytic activity of different heterogeneous catalysts in the cinnamaldehyde hydrogenation

Reference	Material	Condition	Time (h)	Conversion (%)	TOF (h^{-1})*
	This work	EtOH/60ºC/1.2 bar	0.42	97	1663
8	C nanofiber- Pd	Dioxane/80ºC/H2 flow	0.5	100	394.4
9	Pd-WN/SBA-15	Isopropanol/40ºC/10bar	2	70.6	757
10	N-doped carbon-Pd	2-propanol/30ºC/5bar	4	100	390.6
11	N-doped C Nanotubes	Dioxane/80ºC/H2 flow	7.5	90	14.04
12	ZIF-8-Pd	Isopropanol/40ºC/20bar	6	100	70.9
13	C nanotubes/charcoal-Pd	Dioxane/ 70ºC/10bar	2	66.8	716
14	$LaFeO_3$-Pd	cyclohexane/80ºC/10bar	1	90.6	294

*Calculated based on total Pd used in the test

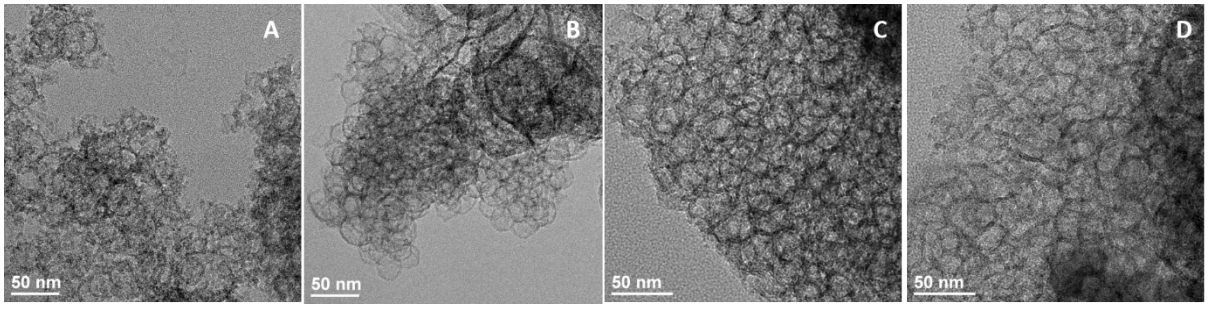

Figure S 27 TEM images of spent MCF-Pd (A,B)and spent MCF-N-IL-Pd (C,D) after 8 cycles of hydrogenation of allylbenzene

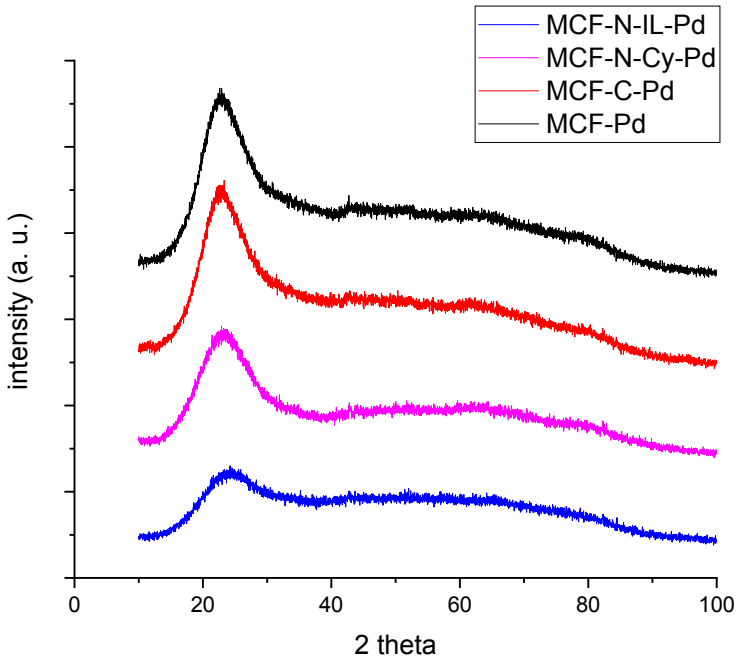

Figure S 28 XRD of spent catalysts after 7 cycles of allylbenzene

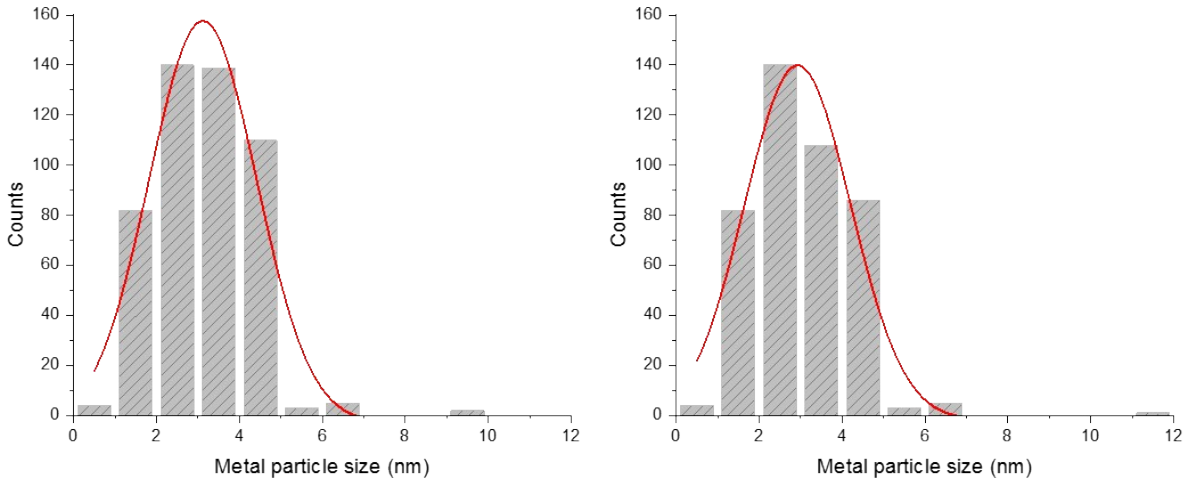

Figure S 29 Histograms of spent MCF-Pd and MCF-N-IL-Pd after 8 cycles of hydrogenation of allylbenzene

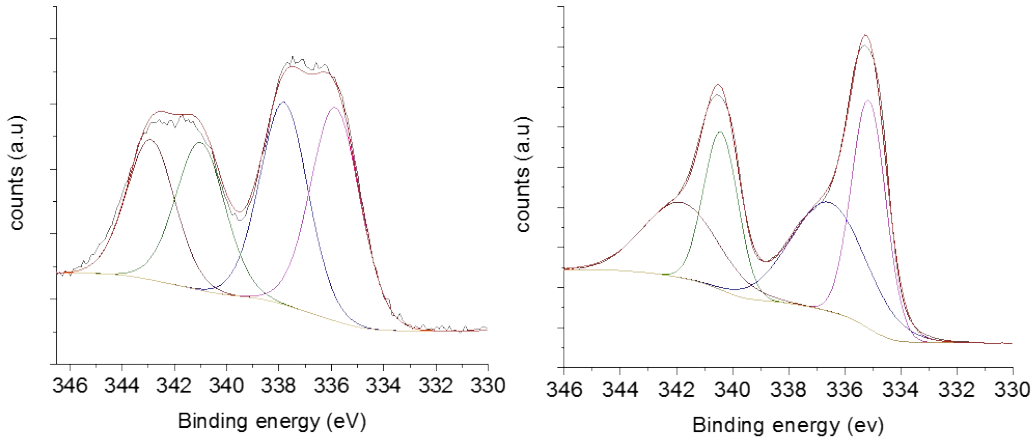

Figure S 30 XPS of MCF-C-Pd before (left) after (right) reduction of Pd species

Table S 10 Relative abundance percentage of palladium types in Pd 3d XPS spectra

sample	Component/BE (eV)	
	Pd^0 335.3	Pd^{2+} 337.5
Pd-MCF-C	50.4%	49.6%
Pd-MCF-C after reduction	72.7%	27.3%

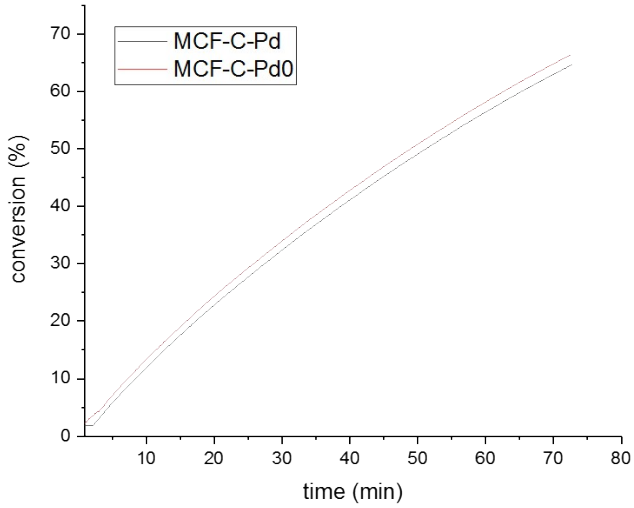

Figure S 31 Catalytic performance of MCF-C-Pd and MCF-C Pd0 reduced with NaBH4

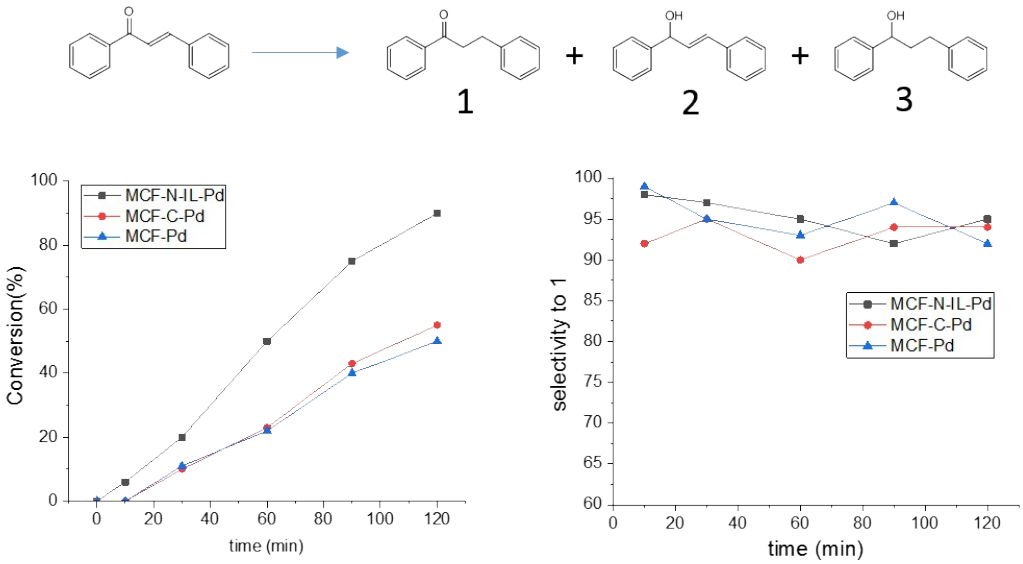

Figure S 32 Hydrogenation of chalcone by synthesized catalysts

4.8 mmols of chalcone, 99 mL of EtOH, 35 mg of catalysts (0.14 % of Pd), 1.2 atm of H_2 and 60ºC

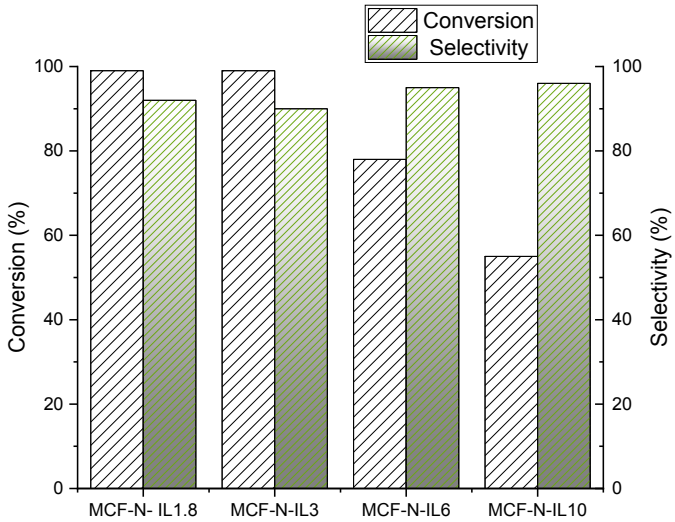

Figure S 33 Influence of N-loading on catalytic activity of hydrogenation of cinnamaldehyde

Table S 11 CO Chemisorption analyses

Sample	Fresh		After Reaction	Spent	
	Pd size (nm)	Dispersion (%)		Pd size (nm)	Dispersion (%)
MCF-Pd	3.6	18	Suzuki	-	-
			Hydrogenation	4.5	19
MCF-C-Pd	3.4	34	Suzuki	25	20
			Hydrogenation	4.5	30

MCF-N-IL-Pd	3.5	38	Suzuki	6.5	32
			Hydrogenation	4.0	37

Table S 12 FWHM for XPS fitting Pd 3d for fresh materials

Sample	Name	FWHM eV
MCF-Pd	Pd3d5 Scan A (335.3 eV)	1.41
	Pd3d5 Scan B (337.5 ev)	2.52
MCF-C-Pd	Pd3d5 Scan A	2.17
	Pd3d5 Scan B	2.22
MCF-N-Cy-Pd	Pd3d5 Scan A	2.08
	Pd3d5 Scan B	1.96
MCF-N-IL-Pd	Pd3d5 Scan A	2.08
	Pd3d5 Scan B	1.96
MCF-N-Ac-Pd	Pd3d5 Scan A	2.02
	Pd3d5 Scan B	3.08

References

1 B. W. Glasspoole, J. D. Webb and C. M. Crudden, *J. Catal.*, 2009, **265**, 148–154.

2 N. J. S. Costa, P. K. Kiyohara, A. L. Monteiro, Y. Coppel, K. Philippot and L. M. Rossi, *J. Catal.*, 2010, **276**, 382–389.

3 R. Fareghi-Alamdari, M. G. Haqiqi and N. Zekri, *New J. Chem.*, 2016, **40**, 1287–1296.

4 C. Putta, V. Sharavath, S. Sarkar and S. Ghosh, *RSC Adv.*, 2015, **5**, 6652–6660.

5 C. Schmöger, T. Szuppa, A. Tied, F. Schneider, A. Stolle and B. Ondruschka, *ChemSusChem*, 2008, **1**, 339–347.

6 J. H. Park, F. Raza, S. J. Jeon, H. I. Kim, T. W. Kang, D. Yim and J. H. Kim, *Tetrahedron Lett.*, 2014, **55**, 3426–3430.

7 B. Cornelio, G. A. Rance, M. Laronze-Cochard, A. Fontana, J. Sapi and A. N. Khlobystov, *J. Mater. Chem. A*, 2013, **1**, 8737–8744.

8 C. Pham-Huu, N. Keller, G. Ehret, L. J. Charbonniere, R. Ziessel and M. J. Ledoux, *J. Mol. Catal. A Chem.*, 2001, **170**, 155–163.

9 D. Wang, Y. Zhu, C. Tian, L. Wang, W. Zhou, Y. Dong, H. Yan and H. Fu, *ChemCatChem*, 2016, **8**, 1718–1726.

10 A. S. Nagpure, L. Gurrala, P. Gogoi and S. V. Chilukuri, *RSC Adv.*, 2016, **6**, 44333–44340.

11 J. Amadou, K. Chizari, M. Houllé, I. Janowska, O. Ersen, D. Bégin and C. Pham-Huu, *Catal. Today*, 2008, **138**, 62–68.

12 Y. Zhao, M. Liu, B. Fan, Y. Chen, W. Lv, N. Lu and R. Li, *Catal. Commun.*, 2014, **57**, 119–123.

13 P. H. Z. Ribeiro, E. Y. Matsubara, J. M. Rosolen, P. M. Donate and R. Gunnella, *J. Mol. Catal. A Chem.*, 2015, **410**, 34–40.

14 S. Bewana, M. J. Ndolomingo, E. Carleschi, B. P. Doyle, R. Meijboom and N. Bingwa, *ACS Appl. Mater. Interfaces*, 2019, acsami.9b10820.